

The Effects of Glycerol on Biofilm Production

Nicholas Nedzesky¹, Abigail Matela[#], Thomas Lavelle[#] and Brian Carson[#]

¹Seneca Valley Senior High School, Harmony, PA, USA

[#]Advisor

ABSTRACT

Due to the widespread, antibiotic-resistant nature of biofilm-producing bacteria, there is high demand for research on biofilm formation. This research serves as a contribution to the existing knowledge of how biofilms form. Its results could shed light on how biofilm-producing bacteria utilize communication pathways in response to environmental and chemical stimuli. To determine the effects of glycerol (a sugar alcohol linked to osmotic stress) on biofilm production, *Pseudomonas fluorescens* strain SBW25 was cultivated within a series of 5 culture tubes containing medias with increasing concentrations of glycerol from 0-10%. After a week of incubation, a sample from each of the tubes was plated and colony morphology was qualitatively analyzed. Each of the tubes was then stained with crystal violet and the absorbance of the biofilm could be quantitatively measured at 590nm with a dual-beam spectrophotometer. The hypothesis is supported with the absorbance and plate data collected over the first and second trials of the experiment. As glycerol concentration increased, the absorbance (and thus biofilm produced) increased proportionately, and the approximate number of wrinkly mutants on each successive plate increased. The correlation of the data is significant enough to support the hypothesis, but more trials will need to be conducted in order to conclusively accept it.

Introduction

Biofilm-producing bacteria are responsible for approximately 65-80% of all human bacterial infections, thus there is high demand for research regarding biofilm formation and the treatment of antibiotic-resistant, biofilm-related bacterial infections (Baker et al., 2016). Biofilms are communities of bacteria encased in an extracellular matrix composed of proteins, extracellular eDNA, and exopolysaccharides.

Glycerol, a sugar alcohol, diffuses in large quantities into cells and thus causes high levels of osmotic stress which compresses cell membranes (Pocivavsek et al., 2011). Glycerol-induced stress would select for mutations within the *wsp* pathway, a pathway found within the periplasm of biofilm-producing bacteria which is responsible for much of the production of cyclic-di-GMP, a secondary signaling molecule critical to cellular communication and biofilm production. Hypothetically, mutants would produce large amounts of cyclic-di-GMP so as to produce more biofilm for protection against osmotic stress. Glycerol-induced membrane compression would also induce this pathway, as the high-stress environment would mechanically stimulate the *wsp* pathway, causing increased cyclic-di-GMP production and thus, increased biofilm production (Arnbruster et al., 2019).

The hypothesis states that if *P. fluorescens* is grown in the presence of increasing concentrations of glycerol, then the biofilm production of the bacteria and the number of wrinkly phenotype mutants should significantly increase. This is because glycerol-induced stress will induce the *wsp* pathway and select for bacteria with mutations which produce more biofilm for protection.

Methods and Procedure

Experimental Setup

5 culture tubes were used in the experiment, each containing a unique recipe of glycerol media created by following the calculated recipes listed in the table below. Appropriate amounts of glycerol, deionized water, proteose peptone no. 3, and K_2HPO_4 dibasic were vortexed then autoclaved at $138^\circ C$ for 45 minutes. .05g $MgSO_4$ was autoclaved at the same temperature for 45 minutes and .01g was added to each tube. Each tube contained 15 mL of media with an increasing glycerol concentration. The tubes with 0% glycerol and 2.5% glycerol were considered controls because of their low concentrations.

Table 1. Media Recipes (Makes 15mL Each).

Glycerol (%)	Glycerol (mL)	Water (mL)	$MgSO_4$ (g)	Prot. no. 3 (g)	K_2HPO_4 (g)
0	0.000	15.000	0.010	0.300	0.022
2.5	0.374	14.626	0.010	0.300	0.022
5.0	0.749	14.251	0.010	0.300	0.022
7.5	1.124	13.876	0.010	0.300	0.022
10.0	1.499	13.501	0.010	0.300	0.022

Plating Procedure

Using an inoculating loop, *Pseudomonas fluorescens* was transferred from an agar stab to 3mL of LB broth and incubated at $28^\circ C$ and 100rpm in an orbital shaker for 1 day. A dilution series was set up by labeling 3 microcentrifuge tubes with 10^{-1} , 10^{-2} , and 10^{-3} . 950 uL of phosphate buffered saline (PBS) was added to the 10^{-1} tube and 900uL PBS was added to the 10^{-2} and 10^{-3} . 50uL from the LB broth was added to the 10^{-1} microcentrifuge tube and vortexed. This was the first dilution at 5% concentration. 100uL from the 10^{-1} tube was added to the 10^{-2} tube. This was the second dilution at .5% concentration. 100uL from the 10^{-2} tube was added to the 10^{-3} tube. This was the third dilution at .05% concentration.

100 uL of the .05% concentration was plated on a 2% agar plate prepared with 100 uL 100 mg/mL 1000x ampicillin stock to reduce plate contamination. This was the ancestral colony control plate and it was incubated upside down at $28^\circ C$ for 1 day.

Tube Transfer and Incubation Procedure

5 more culture tubes were obtained and 2mL of media from each of the original tubes was pipetted into each of the corresponding tubes. Using a sterile inoculating loop, different ancestral bacterial colonies were transferred from the ancestral colony plate to each of the culture tubes.

The culture tubes were incubated on an orbital shaker for 7 days at $28^\circ C$. The tubes were incubated at room temperature (defined as $23^\circ C$ for this experiment) 1 day and 4 through 7 days after inoculation. 2 days after inoculation, 5 more culture tubes were obtained and 1.5mL of each of the appropriate concentrations of media was added to each. 500uL from each original tube was transferred to each of the new tubes and incubated at $28^\circ C$. The transfer process was repeated 2 days after the first transfer. After a week of incubation, the plating procedure was followed to prepare 5 plates, except a 50uL sample from each of the culture tubes was added to 5 corresponding 10^{-1} tubes. 100uL of the .05% concentrations was plated.

Staining Procedure

After a week of incubation, the liquid portion from each culture tube was pipetted out and expelled into a 10% bleach waste container, leaving behind the solid mass of biofilm on the sides and at the bottom of the tubes. While pipetting liquid from these tubes, it was important to be careful not to disturb the biofilms on the sides so as to not break them off and accidentally pipette them out. It was also critical to ensure that all biofilm was stained and able to be measured.

3 mL of .1% crystal violet solution was added to each tube, and an additional empty culture tube was included which acted as a control for any dye that stained the tube itself. These tubes were incubated at room temperature for 1 day.

The crystal violet was pipetted out of every culture tube and expelled into the waste container. The crystal violet was rinsed away by carefully adding 10mL of deionized water to each tube. The tubes were incubated at room temperature for 1 day again, then the liquid was pipetted out from each tube and expelled into the waste container. 15 mL of 95% ethanol solution was added to each tube and vortexed until the stained biofilms completely dissolved. Each tube was diluted to 10% concentration (1mL solution into 9mL ethanol). 2mL from each tube was transferred to three cuvettes. 3 cuvettes for every tube were used to serve as technical replicates.

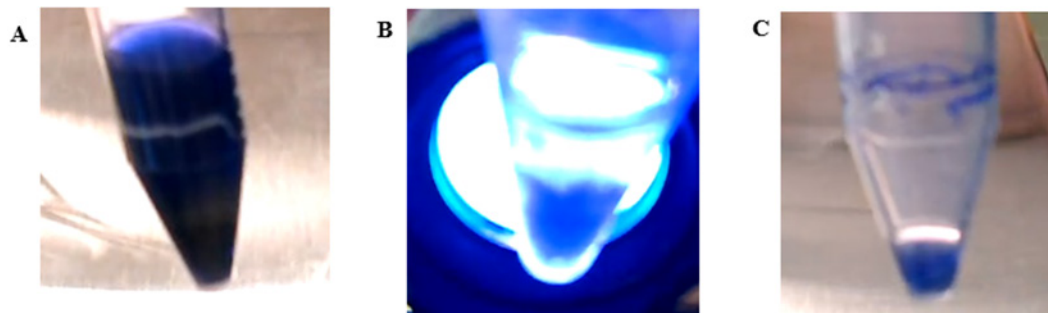


Figure 1. Tubes at Different Steps of the Staining Procedure. Figure 1A shows the first trial 10% tube after adding crystal violet solution. Note the white ring of biofilm growth around the edge of the tube. Figure 1B is the first trial 2.5% tube after rinsing with water, held in front of a UV light. A mass of biofilm can be seen settled at the bottom. Figure 1C is the first trial 7.5% tube before ethanol was added. Note the stained biofilm ring along the edge and the mass at the bottom.

Data Collection

A dual-beam spectrophotometer was used to measure absorbance at 590nm. The results of the plates were photographed and compared qualitatively with the control and ancestral plates. Colony morphology for each plate was documented. The steps of the experiment were repeated for a second trial.

Results

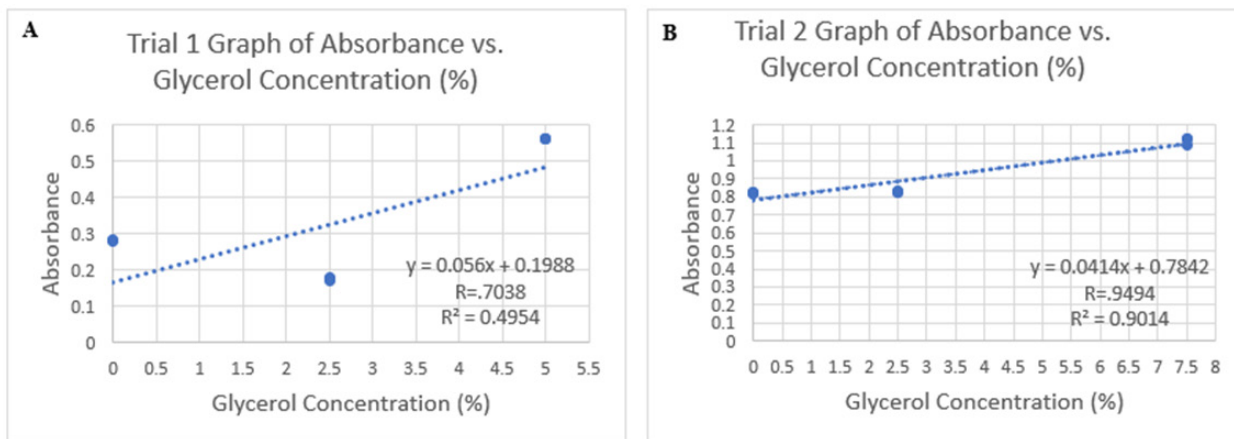
Quantitative Spectrophotometry Data

Table 2. Spectrophotometry Data Including Minimum, Median, and Maximum Readings Per Each Tube.

*These data values are outliers due to error explained later. They are omitted in the statistical analysis.

Figure 2. Graphs of Absorbance vs. Glycerol Concentration for Both Trials. Figure 2A is the graph of the first trial data. Note the positive correlation: $R=.7038$ ($p=.034$). Figure 2B is the graph of the second trial data. Note the positive correlation: $R=.9494$ ($p<.0001$).

All data was collected using a dual-beam spectrophotometer measuring absorbance at 590nm. Three cuvettes were used for each tube in order to document the variability of the instrument. The average standard deviation of each of the technical replicates was .004, which shows miniscule variability between measurements. All data was graphed and the Pearson correlation coefficient along with the coefficient of determination were calculated using



$R = \frac{\sum_{i=1}^n (x_i - \bar{x})(y_i - \bar{y})}{\sqrt{\sum_{i=1}^n (x_i - \bar{x})^2} \sqrt{\sum_{i=1}^n (y_i - \bar{y})^2}}$. The first trial data exhibits poor linear fit $R^2=.4954$, albeit positive correlation $R=.7038$ ($p=.034$). The second trial exhibits both high linear fit $R^2=.9014$ and highly positive correlation $R=.9494$ ($p<.0001$). Correlation significance was determined using $t = \frac{R\sqrt{n-2}}{\sqrt{1-R^2}}$ test statistics and critical values for each trial's data. Both correlations are significant, however trial 1 displays lower significance due to errors explained later in the Error Analysis. All omitted outliers will also be explained in the Error Analysis.

Glycerol Concentration (%)	Absorbance						Transmittance (%)					
	Trial 1			Trial 2			Trial 1			Trial 2		
	Min.	Med.	Max.	Min.	Med.	Max.	Min.	Med.	Max.	Min.	Med.	Max.
0	0.277	0.280	0.284	0.821	0.823	0.824	52.00	52.48	52.84	15.00	15.03	15.10
2.5	0.170	0.177	0.180	0.827	0.830	0.833	66.07	66.53	67.61	14.69	14.79	14.89
5.0	0.560	0.560	0.561	0.576*	0.580*	0.582*	27.48	27.54	27.54	26.18*	26.30*	26.55*
7.5	0.035*	0.040*	0.041*	1.090	1.124	1.127	90.99*	91.20*	92.26*	7.46	7.52	8.13
10.0	0.355*	0.357*	0.358*	Data Unavailable			43.85*	43.95*	44.16*	Data Unavailable		

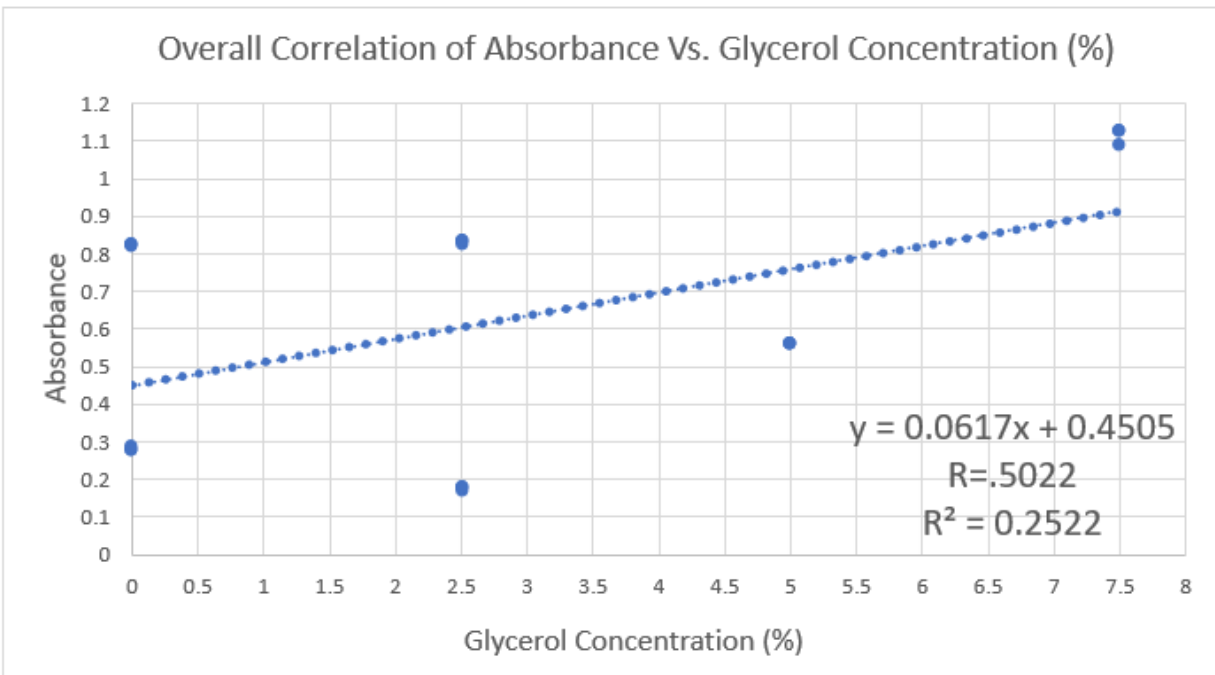


Figure 3. Combined Trial Graph.

Combining both trials into an overall graph will demonstrate an approximate overall correlation meant to summarize the relationship between glycerol concentration and absorbance. The overall regression exhibits low linear fit $R^2 = 0.2522$ and positive correlation $R = .5022$ ($p < .034$). The trial data along with the overall data support the hypothesis because they demonstrate positive correlation. Notably, the overall correlation is not as high as its constituent trials, although it is significant. This demonstrates the need for continued experimentation to illustrate a clearer correlation, which would hypothetically be closer to its constituent trials' correlations.

Qualitative Data

With each increasing concentration of glycerol, there was a visibly higher proportion of wrinkly mutants observed on the plates. Unfortunately, this part of the experiment was limited in that there were too many colonies on each of the plates, thus the number of smooth and wrinkly colonies could not be quantitatively counted but had to be qualitatively observed. With each of the higher concentration plates like 5%, 7.5%, and 10%, there were large regions of primarily wrinkly colonies.

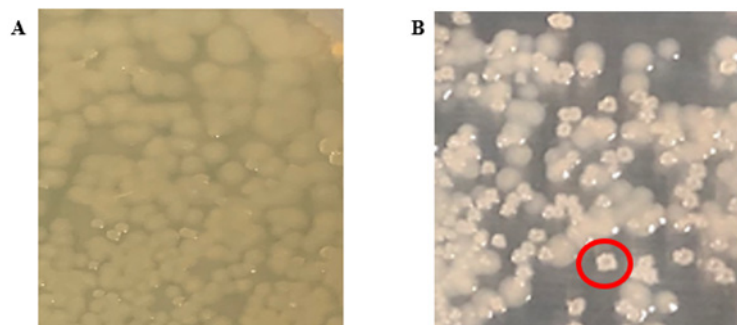


Figure 4. Plate Data. Figure 4A is a sample of the ancestral colony control plate. Note the majority of smooth, round colonies. Figure 4B is a sample of the 2nd trial 10% plate. Note the majority of wrinkly mutants.

The ancestral, 0%, and 2.5% plates had almost all smooth colonies with only a minimal number of wrinkly mutants interspersed throughout (once again making counting difficult). Each successive concentration had visibly larger amounts of wrinkly mutants, and the 5%, 7.5%, and 10% plates had primarily wrinkly colonies with smooth colonies interspersed. They had large patches of mostly wrinkly colonies mentioned earlier. Almost all wrinkly mutants were visibly smaller than smooth colonies although there were some (notably on the 5% second trial plate) which were about the same size, or even larger than an average smooth colony.

In terms of biofilm production within the tubes, the 5%, 7.5%, and 10% tubes each had visibly larger biofilm pellets growing on the bottoms of their tubes compared to the 0% and 2.5% tubes across both trials. There were also rings of biofilm growing around the tube at the media-air interface. There was an impressively large amount of biofilm in the 5% tube. More information will be explained in the Error Analysis, but the 10% tube had actually produced so much biofilm that it was incredibly difficult to stain and analyze. Thus, the 10% tube data was omitted from the experiment for that reason and other reasons to be explained later.

Discussion

The data and statistical analyses above demonstrate that there is growing support for the hypothesis provided in the Introduction. There was significant, positive correlation between glycerol concentration and absorbance, which is used in this experiment as a measure of biofilm production. Increased absorbance is due to the presence of more stained biofilm, thus the tube with the largest absorbance, the 2nd trial 7.5% tube, produced the most biofilm as measured. The positive correlation between the glycerol concentration and the measured absorbance illustrates that as glycerol concentration increases, the absorbance, and thus amount of biofilm produced, tends to increase proportionately. This is in line with the expectations defined in the hypothesis, supporting the theory that glycerol induces the *wsp* pathway which causes an increase in biofilm production. Additionally, visibly larger amounts of wrinkly mutants were present in each successive plate, supporting the natural selection aspect of the hypothesis as well. Based on the results of the experiment, glycerol could indeed act as a selection factor for high biofilm producing wrinkly mutants. The significance of this data is enough to support the hypothesis, although more trials will have to be run in order to obtain more conclusive results on the effects of glycerol on biofilm production.

Error Analysis and Limitations

As with all research, this experiment was subject to a variety of errors, especially due to COVID-19 related circumstances. Research was not always able to be performed on certain days, due to the fact that this experiment was performed in a school lab which was subject to closures because of elevated COVID-19 cases in the school. Thus,

the second trial differed slightly from the first in that the tube transfer procedure was only followed once and not twice due to time constraints. This contributes to the variability between the correlations. Additionally, the stain in the tubes was allowed to sit for an additional day, which contributed to the overall higher absorbance readings compared to the first trial. This should not affect the significance of the results examined in this experiment, however, because the consistency of staining within each trial preserves the accuracy of the correlations and the significance of the data.

The staining itself also produced error, as some biofilm unstained for uncontrollable reasons, producing absorbance values lower than if all the biofilm had stained properly. This could possibly be due to the fact that *P. fluorescens* is gram-negative and thus retains stain poorly. Data from tubes which had unstained was omitted in the graphs and the statistical analyses, as this data contained outliers due to error. The second trial 5% tube, first trial 7.5% tube, and first trial 10% tube all experienced various amounts of unstaining. As mentioned earlier, the first trial 10% tube had actually produced so much biofilm around the edges of the tube that not all of it could be stained. Hypothetically, the 10% tube should have had the most biofilm growth, and it did in fact exhibit large amounts of growth. However, more data will need to be collected to confirm this and a more refined staining procedure will need to be used in order to stain all the biofilm present. The second trial 10% tube was lost to an uncontrollable error. In an attempt to modify the staining procedure to ensure all 10% biofilm could be stained, a centrifuge was used. The centrifuge turned out to be faulty and it severely damaged the tube.

Additionally, one of the limitations of this experiment was that the plated colonies were not diluted enough to be able to quantitatively count the mutants. In future trials, a greater dilution factor will be used.

Conclusion

The hypothesis was supported by the data collected in this experiment, however more trials need to be conducted in order to fully accept it. The positive correlations between glycerol concentration and biofilm production, along with the observed increase of wrinkly colony mutants across the plates all suggest that glycerol is both an inducer of the *wsp* pathway and a selection factor for the bacteria which produce the most biofilm. These results shed light on how biofilm producing bacteria respond to osmotic stress through the production of biofilm. More experimentation on the *wsp* pathway and other communication pathways could be explored in the future, along with other solutes which create osmotic stress. Understanding what promotes the biofilm-producing pathways within these bacteria could help in understanding how to inhibit the production of biofilm, an important topic within biofilm research. Overall, this experiment's hypothesis was supported by the data collected, and there are promising applications of this data to future research.

Acknowledgments

A special thanks to Dr. Matela for answering my numerous questions and providing mentorship during the setup of the experiment. She provided valuable feedback about the procedure of the experiment and an incredible opportunity for me to present my research to staff from her lab. A huge thank you to Mr. Lavelle and the Mr. Carson, the directors of the laboratory in which this experiment was performed. Without them, this research could not have been completed during the COVID-19 pandemic. On days that the school was closed to students due to elevated COVID-19 cases, Mr. Lavelle and Mr. Carson would provide necessary help in order to complete certain time dependent steps like tube transfers. During a period of remote virtual learning, Mr. Carson helped perform various steps of the first trial of the experiment while I instructed over Microsoft Teams. This project would not be feasible without both of their dedication in the laboratory and without their resourcefulness during trying times.

References

1. Armbruster, C. R., Lee, C. K., Parker-Gilham, J., de Anda, J., Xia, A., Zhao, K., Murakami, K., Shan Tseng, B., Hoffman, L. R., Jin, F., Harwood, C. S., Wong, G. C., & Parsek, M. R. (2019). Heterogeneity in Surface Sensing Suggests a Division of Labor in *Pseudomonas aeruginosa* Populations. *eLife*. <https://doi.org/10.7554/eLife.45084>
2. Baker, P., Hill, P. J., Snarr, B. D., Alnabelseya, N., Pestrak, M. J., Lee, M. J., Jennings, L. K., Tam, J., Melnyk, R. A., Parsek, M. R., Sheppard, D. C., Wozniak, D. J., & Howell, P. L. (2016). Exopolysaccharide Biosynthetic Glycoside Hydrolases Can Be Utilized to Disrupt and Prevent *Pseudomonas aeruginosa* Biofilms. *Science Advances*, 2(5). <https://doi.org/10.1126/sciadv.1501632>
3. Chen AI, Dolben EF, Okegbe C, Harty CE, Golub Y, et al. (2014) *Candida albicans* Ethanol Stimulates *Pseudomonas aeruginosa* WspR-Controlled Biofilm Formation as Part of a Cyclic Relationship Involving Phenazines. *PLOS Pathogens* 10(10): e1004480. <https://doi.org/10.1371/journal.ppat.1004480>
4. Ferreira, R., Ferreira, M., Glatthardt, T., Silvério, M. P., Chamon, R. C., Salgueiro, V. C., Guimarães, L. C., Alves, E. S., & Dos Santos, K. (2019). Osmotic Stress Induces Biofilm Production by *Staphylococcus epidermidis* Isolates from Neonates. *Diagnostic microbiology and infectious disease*, 94(4), 337–341. <https://doi.org/10.1016/j.diagmicrobio.2019.02.009>
5. Haas, D., & Keel, C. (2003). Regulation of Antibiotic Production in Root-Colonizing *Pseudomonas* spp. and Relevance for Biological Control of Plant Disease. *Annual Reviews*, 41(117-153). <https://doi.org/10.1146/annurev.phyto.41.052002.095656>
6. Matela, A. (2020). EvolvingSTEM bioinformatics module. In A. Matela (Author), *EvolvingSTEM bioinformatics module*. EvolvingSTEM.
7. Pocivavsek, L., Gavrilov, K., Cao, K. D., Chi, E. Y., Li, D., Lin, B., Meron, M., Majewski, J., & Lee, K. Y. (2011). Glycerol-Induced Membrane Stiffening: the Role of Viscous Fluid Adlayers. *Biophysical journal*, 101(1), 118–127. <https://doi.org/10.1016/j.bpj.2011.05.036>
8. Suma C. Pemmaraju, Kumar Padmapriya, Parul A. Pruthi, R. Prasad & Vikas Pruthi (2016) Impact of Oxidative and Osmotic Stresses on *Candida albicans* Biofilm Formation, Biofouling, 32:8, 897-909, <https://doi.org/10.1080/08927014.2016.1212021>